A Sector Array using Dielectric Loaded Antennas at 60GHz

Takeshi OHNO and Koichi OGAWA

Communication Devices Development Center, Matsushita Electric Industrial Corporation Limited

Kadoma 1006, Kadoma City, Osaka, 571-8501 Japan

Phone: +81-6-6900-9613, Fax: +81-6-6900-9614, E-mail: ohno.ken@jp.panasonic.com

1. Introduction

There has recently been growing interest in high-speed communications at 60GHz. Among the various applications that could achieve this aim, a short-range indoor wireless LAN for data transmission at over-Giga-bit rates (such as studio quality non-compressed digital HDTV) is a promising candidate due to its high level of allocated frequency resources.

There are some difficulties in realizing millimeter wave communications, such as a large propagation loss and high thermal noise due to the wide frequency bandwidth needed for high-capacity data transmission. These results in a smaller C/N value than would be found in a system used for lower frequencies. Therefore, the gain of the antennas used in such equipment has to be large to meet the required C/N for obtaining a predetermined transmission quality.

For indoor applications, the antenna also needs to have a broad radiation pattern so that communications can be carried out at arbitrary locations in a room. However, there is a theoretical relationship between the gain and the beam width of an antenna, indicating that a broader beam width leads to lower gain.

To overcome these difficulties, we have attempted to introduce a sector array using dielectric loaded antennas [1], [2]. The antenna gives a radiation pattern in which the main beam points off-axis from the broadside direction, while maintaining a sectorial radiation pattern in which the radiation intensity remains almost unchanged over a specified solid angle where we expect the communication to be conducted [3].

The antenna presented in this paper is intended for use inside buildings, and therefore it needs to achieve a coverage area or spatial availability in a room where communications are to be performed with acceptable transmission quality. Hence, an evaluation with regard to the spatial coverage has been carried out by means of measuring the three-dimensional radiation patterns of the sector array over the whole solid angle [4]. From this work, we have clarified that the performance of the antenna fulfills the system criteria based on outage considerations.

2. Formation of a Sector radiation pattern

2.1 Antenna Configuration

The dielectric loaded antenna was initially designed to receive broadcast satellite signals [1]. The antenna includes a dielectric with a pillar-like structure and has radiation patterns with a narrow beamwidth aligned in the broadside direction [1]. Our objective however, is to create a sectorial radiation pattern with an inclination from the broadside direction. Thus, we have attempted some modification of the shape of the dielectric to achieve this end.

Fig. 1 shows the configuration of a single antenna element. A dielectric material made of polypropylene with a permittivity of 2.26 is mounted on the aperture of an ordinary rectangular waveguide. The dielectric is 6.9mm in height with a diameter of 6.1mm. The top surface of the dielectric is cut in the yz-plane, as shown in Fig. 1, where the cutting-angle on the top surface is α. The dielectric is located on the aperture and displaced in the direction of the y-axis, where the distance between the center of the dielectric and that of the aperture is p [3], [5]. By incorporating these two operations, the main beam is tilted in the opposite direction to the slope of the dielectric while maintaining s sectorial radiation pattern, as explained in the next section.

2.2 Experimental Results

In the first step of our investigation, the variation in the radiation pattern with α and p was measured. Figs. 2 and 3 show the variation in the main beam direction θ_0 with α (p = 0) and p ($\alpha = 0^\circ$ and 45°) as parameters. These figures indicate that the main beam direction increases rapidly when α is more than 15° and that it increases in proportion to p.

Fig. 4 shows the radiation patterns for $\alpha = 30^\circ$ and 45° (p = 0), and for p = 1.0mm and 1.7mm ($\alpha = 45^\circ$).

ISBN: 4-88552-207-2 C3055©IEICE

The figure shows a change in α causes the main beam to be skewed from the broadside direction and a change in p allows the beam width to be enlarged. By combining these two properties, a sector radiation pattern that is in alignment and with a gain of 10dBi can be obtained under the condition where $\alpha = 45^\circ$ and p = 1.7mm.

2.3 Consideration of the Principle

Consideration is now given to a high frequency technique known as 'geometrical optics' or the 'ray trace method'. In the calculations, the electromagnetic field distributing from the waveguide aperture is considered as be a single point source for the sake of simplicity.

Fig. 5(a) shows the calculated results for the distribution of the rays. The figure suggests that most of the rays traveling through the dielectric concentrate on the positive direction of the y-axis. The significant rays for $\theta = 20^\circ$, 40°, 60° and 80° are extracted from Fig. 5(a) and shown in Fig. 5(b). It was found that two rays exist at each angle, where electromagnetic waves that travel with different paths propagate in the dielectric. By calculating the path of each pair of rays, the composition of the electric field E can be calculated from the following equation:

$$E(\theta) = T_1 \exp(-j\varphi_1) + T_2 \exp(-j\varphi_2) \quad (1)$$

where T and φ are the transmission coefficient and the phase delay effected by the path of the ray.

Fig. 6 shows the electric field calculated by Eq. (1). It can be seen that the magnitude of E is nearly constant between 20° and 60°, and that the flatness of the sector radiation pattern is formed in this angular region.

3 Sector Array

3.1 Measurement of 3D-Radiation Patterns

The structure of a 4-sector array is shown in Fig. 7. The 4-sector array was constructed by locating the dielectric antenna (as described in the previous section) on the positive and negative directions of the x and y-axes. The distance between the dielectrics was set to be 1.1mm.

The sectorial method described in this paper, in which a coverage area is spatially divided using plural antenna elements, has the disadvantage that there is a crossover property between the elements whereby the communication might fail to connect due to weak signal strength. Thus, an evaluation of this crossover is very important from the system design viewpoint. However, it is difficult to determine the accurate crossover value at a particular angle of interest by using the 2-dimensional radiation pattern (such as Fig. 4) since the two radiation patterns emitted from the adjacent sectors create complicated boundaries in their border region. Therefore, we measured 3-dimensional radiation patterns using the apparatus shown in Fig. 8 [6].

Fig. 9 shows the measured 3D-radiation pattern of a single sector antenna element under horizontal polarization (φ–pol.). The composition of the measured 3D-radiation pattern for the 4-sector array is shown in Fig. 10.

It was confirmed that the sector radiation pattern is formed in four directions and that the crossover depth between the elements is as large as 28dB because of the relatively narrow beam width in the horizontal plane.

3.2 Evaluation of Spatial Coverage

As described in the previous section, the developed sector array has a large crossover. From the system design viewpoint, we need to evaluate how this crossover characteristic effects the area of coverage where communications can be performed. Hence, we introduce an estimation criterion for the system, referred to as the spatial coverage η, which is defined as

$$\eta(\theta_H, \theta_V) = \frac{\int_{\theta_\alpha}^{\theta_\beta} \sin\theta d\theta \int_{\varphi_\alpha}^{\varphi_\beta} d\varphi}{2\int_{\theta_H}^{\theta_V} \sin\theta d\theta \int_0^{\pi} d\varphi} = \frac{(\cos\theta_\beta - \cos\theta_\alpha)(\varphi_\beta - \varphi_\alpha)}{2\pi(\cos\theta_V - \cos\theta_H)} \quad (2)$$

where the numerator indicates that, from θ_α to θ_β and from φ_α to φ_β, the measured gain satisfies the system requirements. The denominator represents the solid angle where communication is supposed to be carried out [4].

Eq. (2) assumes that the base station is installed on a wall and the terminal is located on a desk inside the room, as shown in Fig. 11. In this situation, the terminal antenna does not need to radiate in the vertical direction ($\theta = 0^\circ$ to θ_V) or the horizontal direction ($\theta = \theta_H$ to 90°).

Fig. 12 shows the calculated value of η as a function of the radiation area ($\theta_V - \theta_H$) using the 3D-radiation pattern shown in Fig. 10 when $\theta_H = 20^\circ$ and the required gain is 0, 5, or 10dBi. Fig. 12 shows that η is approximately 90, 70, and 10 % for gains of 0, 5 and 10dBi. This suggests that if we want to cover the room with $\eta = 70\%$, we need to design the gain of the terminal antenna to be 5dBi in the communication link calculation.

The spatial coverage based on the 3D-radiation pattern can clarify the relationship between the antenna performance and the system requirements, and thus is particularly useful in the design of indoor communication systems.

Acknowledgment

The authors would like to thank Dr. T. Tsugawa, former assistant professor of the Osaka Institute of Technology, for his encouragement and support.

References

[1] T. Tsugawa, et al, IEICE Trans., Vol. E73, No.1, pp.128-pp.130, Jan. 1990.

[2] K. Ogawa and T. Uwano, IEICE Trans. Electron., vol. E79-C, no. 5, pp. 685-692, May 1996.

[3] T. Ohno and K. Ogawa, Communications Society Conference of IEICE, B-1-178, Mar. 2003.

[4] T. Ohno and K. Ogawa, Communications Society Conference of IEICE, B-1-85, Mar. 2004.

[5] T. Tsugawa, et al, Communications Society Conference of IEICE, B-121, 1992.

[6] K. Ogawa, et al, Technical Report of IEICE, AP2000-139, pp. 25-32 Nov. 2000.

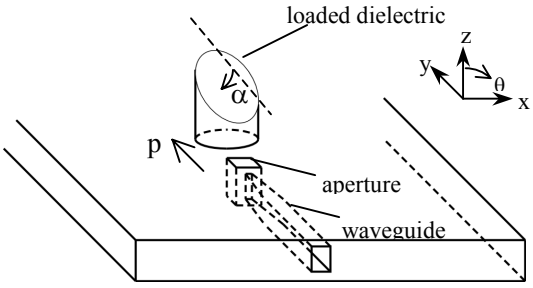

Fig. 1 Structure of the dielectric loaded antenna

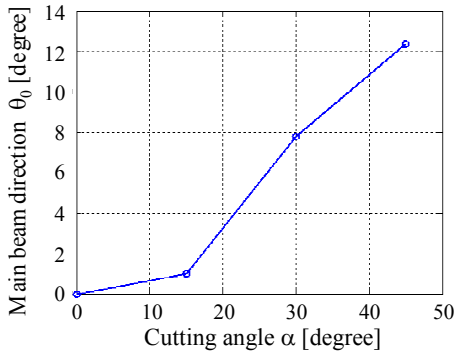

Fig. 2 Main beam direction as function of the tilt angle

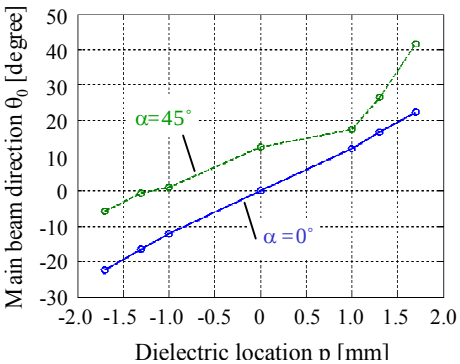

Fig. 3 Main beam direction as function of the dielectric location

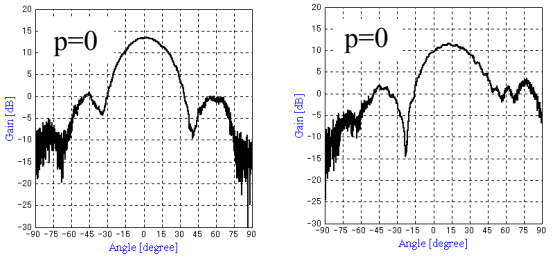

(a) α = 30° (b) α = 45°

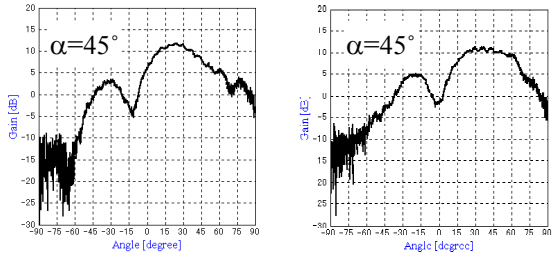

(c) p = 1.0mm (d) p = 1.7mm

Fig. 4 Measured radiation pattern in the yz-plane

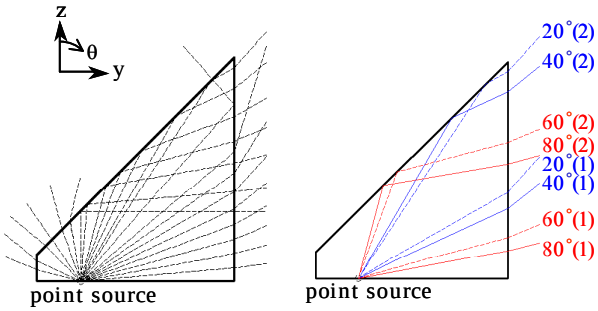

(a) Distribution (b) Significant ray

Fig.5 Ray distribution

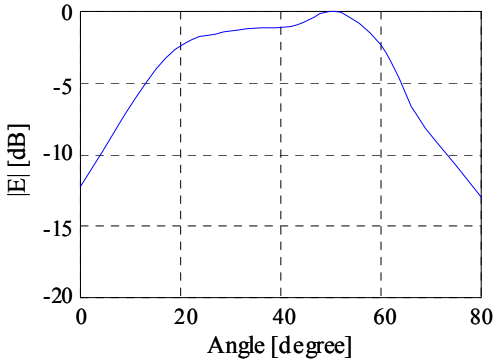

Fig. 6 Calculated electric field

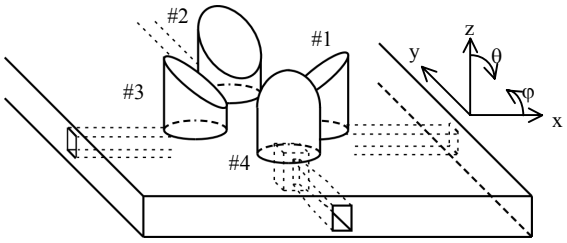

Fig. 7 Structure of the sector array

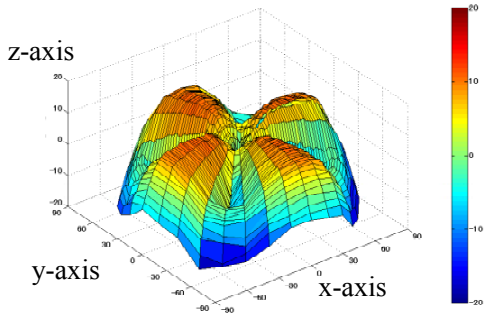

Fig. 10 Measured 3-D radiation pattern of the sector array

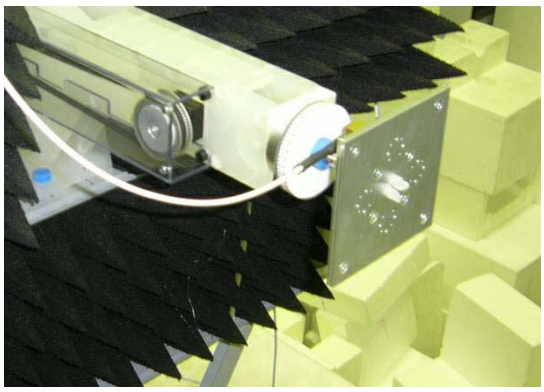

Fig. 8 Apparatus for the measurement of 3D-radation pattern

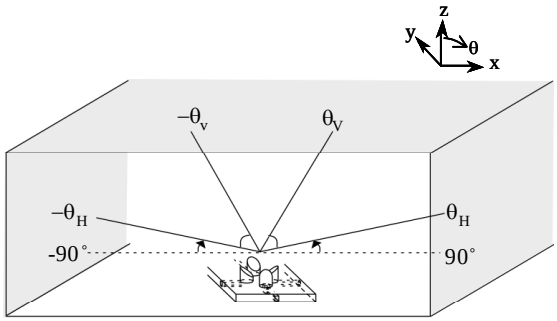

Fig. 11 Radiation direction for the terminal antenna

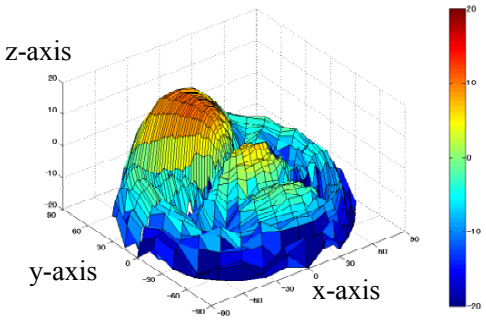

Fig. 9 Measured 3D-radiation pattern of the single sector element

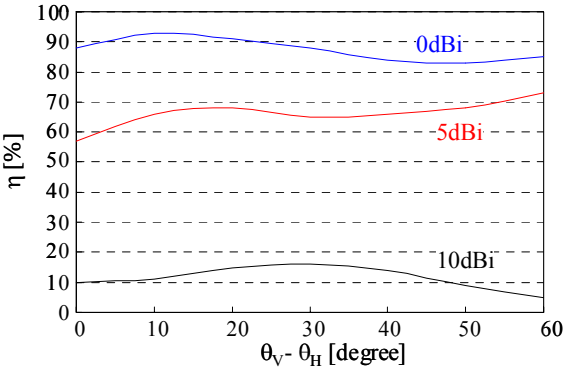

Fig. 12 Calculated spatial coverage